Neurobiology of Disease 144 (2020) 105044

Contents lists available at ScienceDirect

Neurobiology of Disease

journal homepage: www.elsevier.com/locate/ynbdi

Striatal and nigral muscarinic type 1 and type 4 receptors modulate levodopa-induced dyskinesia and striato-nigral pathway activation in 6-hydroxydopamine hemilesioned rats

Alberto Brugnoli, Clarissa Anna Pisanò, Michele Morari*

Department of Biomedical and Specialty Surgical Sciences, Section of Pharmacology, University of Ferrara, 44122 Ferrara, Italy

ARTICLE INFO

Keywords:
Parkinson's disease
Levodopa
Dyskinesia
Muscarinic receptors
Microdialysis
Movement disorders

ABSTRACT

Acetylcholine muscarinic receptors (mAChRs) contribute to both the facilitation and inhibition of levodopa-induced dyskinesia operated by striatal cholinergic interneurons, although the receptor subtypes involved remain elusive. Cholinergic afferents from the midbrain also innervate the substantia nigra reticulata, although the role of nigral mAChRs in levodopa-induced dyskinesia is unknown. Here, we investigate whether striatal and nigral M1 and/or M4 mAChRs modulate dyskinesia and the underlying striato-nigral GABAergic pathway activation in 6-hydroxydopamine hemilesioned rats. Reverse microdialysis allowed to deliver the mAChR antagonists telenzepine (M1 subtype preferring), PD-102807 and tropicamide (M4 subtype preferring), as well as the selective M4 mAChR positive allosteric modulator VU0152100 in striatum or substantia nigra, while levodopa was administered systemically. Dyskinetic movements were monitored along with nigral GABA (and glutamate) and striatal glutamate dialysate levels, taken as neurochemical correlates of striato-nigral pathway and cortico-basal ganglia-thalamo-cortical loop activation. We observed that intrastriatal telenzepine, PD-102807 and tropicamide alleviated dyskinesia and inhibited nigral GABA and striatal glutamate release. This was partially replicated by intrastriatal VU0152100. The M2 subtype preferring antagonist AFDX-116, used to elevate striatal acetylcholine levels, blocked the behavioral and neurochemical effects of PD-102807. Intranigral VU0152100 prevented levodopa-induced dyskinesia and its neurochemical correlates whereas PD-102807 was ineffective. These results suggest that striatal, likely postsynaptic, M1 mAChRs facilitate dyskinesia and striato-nigral pathway activation in vivo. Conversely, striatal M4 mAChRs can both facilitate and inhibit dyskinesia, possibly depending on their localization. Potentiation of striatal and nigral M4 mAChR transmission leads to powerful multilevel inhibition of striato-nigral pathway and attenuation of dyskinesia.

1. Introduction

The contribution of striatal cholinergic interneurons (ChIs) to striatal functions and parkinsonism has long been recognized (Calabresi et al., 2000; Pisani et al., 2007). In the last decade, the role of striatal ChIs in levodopa (L-DOPA) induced dyskinesia (LID) has also emerged (Bordia and Perez, 2019; Moehle and Conn, 2019). Dyskinesia is a major side-effect of L-DOPA pharmacotherapy of Parkinson's disease (PD), and is clinically characterized by abnormal involuntary movements (AIMs) of dystonic and choreic nature (Bastide et al., 2015; Espay et al., 2018). LID has a complex and partially unknown etiology, but the final neurobiological event is the sensitization of D1 receptor expressing striato-nigral GABAergic medium-sized spiny neurons (MSNs) to L-DOPA (Bastide et al., 2015). Striatal ChIs profusely innervate both striato-pallidal and striato-nigral MSNs and influence their activity directly or indirectly, via modulation of dopamine, serotonin, glutamate (Glu) release from striatal afferents, and GABA release from striatal interneurons. Striatal ChIs play a role in LID although the original findings that ablation or functional inhibition of ChIs attenuate LID (Ding et al., 2011; Won et al., 2014) were complemented by a more

Abbreviations: AIMs, Abnormal Involuntary Movements; ALO, Axial, Limb, Orolingual; AP, antero-posterior; AUC, area-under-the-curve; BG, basal ganglia; ChIs, cholinergic interneurons; DA, dopamine; DLS, dorsolateral striatum; DV, dorso-ventral; Glu, glutamate; levodopa, L-DOPA; LID, levodopa-induced dyskinesia; mAChR, acetylcholine muscarinic receptors; ML, medio-lateral; nAChR, acetylcholine nicotinic receptors; PAM, positive allosteric modulator; PPN, pedunculopontine nucleus; 6-OHDA, 6-hydroxydopamine; PD, Parkinson's disease; SNr, substantia nigra pars reticulata; TH, tyrosine hydroxylase

* Corresponding authoe at: Department of Biomedical and Specialty Surgical Sciences, Section of Pharmacology, University of Ferrara, via Fossato di Mortara 17-19, 44121 Ferrara, Italy.

E-mail address: m.morari@unife.it (M. Morari).

https://doi.org/10.1016/j.nbd.2020.105044
Received 4 June 2020; Received in revised form 15 July 2020; Accepted 8 August 2020
Available online 13 August 2020

recent optogenetic study showing that ChIs facilitate LID at low firing rates and attenuating it at higher ones (Bordia et al., 2016). Pharmacological studies showed that both acetylcholine muscarinic receptors (mAChRs) (Bordia et al., 2016; Chambers et al., 2019; Ding et al., 2011; Shen et al., 2015) and acetylcholine nicotinic receptors (nAChRs) (Quik et al., 2015) are involved in LID. However, while it has been convincingly demonstrated that nAChR blockade (with receptor antagonists) or nAChR desensitization (with receptor agonists) prevents LID (Quik et al., 2015), the role of mAChRs is far from clear (Bordia and Perez, 2019). This might be due to the different neuronal distribution and functional roles of mAChR subtypes. In fact, mAChRs are GPCRs grouped in two major families which couple to $G_{i/o}$ (M2 and M4 subtypes) or $G_{q/11}$ (M1, M3 and M5 subtypes), and are unevenly distributed on the different populations of striatal neurons and nerve terminals. In particular, striato-pallidal MSNs predominantly express M1 mAChRs, while striato-nigral MSNs express both M1 and M4 mAChRs (Bernard et al., 1992; Hersch et al., 1994). The M4 subtype is considered the main autoreceptor type at striatal ChIs (Zhang et al., 2002), although also M2 autoreceptors contribute to negative auto feed-back (Bonsi et al., 2008). Another major problem in dissecting out the role of endogenous ACh and mAChR subtypes in LID is the poor selectivity of muscarinic antagonists available. Thus, the unselective muscarinic antagonists dicyclomine and atropine prevented LID in 6-hydroxydopamine (6-OHDA) hemilesioned mice (Bordia et al., 2016; Ding et al., 2011) whereas atropine also prevented LID inhibition induced by optogenetic elevation of ChIs firing rates (Bordia et al., 2016). M4 selective positive allosteric modulators (PAMs) reduced LID in murine and non-human primate models of LID, pointing out a crucial role of M4 mAChRs in this movement disorder (Shen et al., 2015). In partial agreement with this view, the M4 mAChR preferring antagonist tropicamide (Lazareno and Birdsall, 1993; Lazareno et al., 1990) worsened the dyskinetic movements induced by L-DOPA but attenuated those induced by a D1 receptor agonist in 6-OHDA hemilesioned rats (Chambers et al., 2019), suggesting the involvement of different subsets of M4 mAChRs. However, the selectivity of tropicamide for M4 mAChRs has been questioned (Croy et al., 2016), calling for a re-evaluation of its effects with relatively more selective compounds. Finally, the role of ACh in LID might extend beyond striatal ChIs. In fact, cholinergic inputs from the pedunculopontine tegmental nucleus (PPN) to substantia nigra (SN) modulate basal ganglia function (Xiao et al., 2016), and D1 signaling at striato-nigral MSN terminals (Moehle et al., 2017). Although a preliminary report showed that injection of tropicamide in PPN did not modulate LID expression (Chambers et al., 2019), whether M4 mAChRs in SN reticulata (SNr) shape LID remains to be established.

In the present study, in vivo dual probe microdialysis was used to dissect out the role of striatal and nigral M1 and M4 mAChRs in LID and underlying striato-nigral pathway activation. A reverse microdialysis approach was adopted to deliver the M1 mAChR preferring antagonist telenzepine, the M4 mAChR preferring antagonists PD-102807 and tropicamide, and the M4 mAChR selective PAM VU0152100 in dorsolateral striatum or SNr, concurrently with systemic L-DOPA administration. This approach had the two-fold advantage of i) targeting mAChRs in specific brain areas, ii) minimizing the poor selectivity of mAChR antagonists by setting pharmacological selective concentrations in the perfusion Ringer (see Methods). Dyskinetic behavior was monitored concurrently with GABA release in SNr, a readout of striato-nigral MSN activation (Marti et al., 2012; Mela et al., 2012; Mela et al., 2007), and Glu release in striatum, a possible index of cortico-basal ganglia-thalamo-cortical loop activation (Mark et al., 2004; Marti et al., 2005; Marti et al., 2007). The feasibility of this approach was previously demonstrated by showing that reverse dialysis of the D1 receptor antagonist SCH23390, but not the D2 receptor antagonist raclopride, in striatum prevented LID and its neurochemical correlates (Mela et al., 2012).

2. Materials and methods

2.1. Animal subjects

Experimental procedures involving the use of animals complied with the ARRIVE guidelines, and EU Directive 2010/63/EU for animal experiments. Male Sprague-Dawley rats (Charles River Lab, Calco, Lecco; Italy) were housed in a standard facility with free access to food (4RF21 standard diet; Mucedola, Settimo Milanese, Milan, Italy) and water, and kept under regular lighting conditions (12 h dark/light cycle). Animals were housed in groups of two in an 850 cm^2 polysulfone cage (OptiRat; Animal Care Systems, Centennial, CO, USA) with a Scobis Uno bedding (Mucedola, Settimo Milanese, Milan, Italy) and environmental enrichments. Adequate measures were taken to minimize animal pain and discomfort. Experimental protocols were approved by the Ethical Committee of the University of Ferrara and the Italian Ministry of Health (license 170/2013-B).

2.2. Unilateral 6-OHDA lesion

One hundred thirty-two (132) rats (150 g) were unilaterally injected in the (right) medial forebrain bundle with 8 μg of 6-OHDA hydrobromide (dissolved in 0.02% ascorbate-saline), according to the following stereotaxic coordinates from bregma and the dural surface (in mm): antero-posterior (AP) -4.4, medio-lateral (ML) 1.2, dorso-ventral (DV) -7.8, tooth bar at −2.4 mm (Paxinos and Watson, 1986), as previously described (Mela et al., 2012; Morari et al., 1996; Paolone et al., 2015). Animals were pretreated with antibiotics (Synulox™, 50 μl/Kg, i.p.). The wound was sutured and infiltrated with 2% lidocaine solution (Esteve™). Two weeks later, rats were screened by assessing the motor asymmetry score in two different ethological tests (the bar and drag tests) (Pisanò et al., 2020). Rats showing immobility time $>$ 20 s at the contralateral paw in the bar test, and $<$ 3 steps at the contralateral paw (or alternatively a contralateral/ipsilateral paw ratio $<$ 50%) were enrolled in the study (Pisanò et al., 2020).

2.2.1. Microdialysis experiments

Dual probe microdialysis was performed as previously described (Mela et al., 2012; Morari et al., 1996; Paolone et al., 2015). Concentric microdialysis probes were constructed using AN69 semipermeable hollow membranes (65 kDa molecular weight cut-off, 340 μm outer diameter; Gambro Industries, Meyzieu, France). Ninety-six (96) 6-OHDA fully dyskinetic rats (AIMs $>$ 100) obtained after the 21-day priming with L-DOPA were addressed to surgery, so treatment groups were relatively homogeneous in terms of dyskinetic behavior (Supplementary Fig. 1). Even if AIM evaluation in the microdialysis setting (i.e. 24–48 h after surgery) revealed a reduction in limb and axial AIM scores when the response to L-DOPA was compared in the same group of rats at the end of the 21-day L-DOPA treatment (Bido et al., 2011), the degree of dyskinesia severity remained relatively similar across treatment groups also after surgery (Supplementary Fig. 1). One microdialysis probe was stereotactically implanted under isoflurane anesthesia in the dopamine (DA) depleted dorsolateral striatum and another in the ipsilateral SNr. Implantation coordinates from bregma and the dural surface (in mm) (Paxinos and Watson, 1986), and dialysis membrane lengths were: dorsolateral striatum, AP +1.0, ML ± 3.5, DV -6.0 (3 mm), SNr, AP -5.5, ML ± 2.2, DV -8.3 (1 mm). Twenty-four hours after surgery, probes were perfused with a modified Ringer solution ($CaCl_2$ 1.2 mM; KCl 2.7 mM; NaCl 148 mM; $MgCl_2$ 0.85 mM) at a 3 μl/min flow rate. Sample collection (every 20 min) started after 6 h rinsing. At least four baseline samples were collected, then treatments were administered in a randomized fashion (see Experimental design). At the end of experiment, animals were sacrificed by an overdose of isoflurane, and the correct placement of the probes was verified histologically. Severe ($>$ 90%) DA depletion was randomly confirmed by post-mortem Western analysis of tyrosine hydroxylase (TH) levels

(optical density of TH band normalized over α-tubulin: 0.22 ± 0.04 vs 3.13 ± 0.39 lesioned vs unlesioned striatum, respectively, $t = 7.37$ df = 19, Student's *t*-test, two-tailed for paired data; $n = 20$ rats; Supplementary Fig. 2).

2.3. LID induction and AIM ratings

6-OHDA hemilesioned rats received 6 mg/Kg L-DOPA (plus 12 mg/Kg benserazide, s.c.), once a day for 21 days, as originally described by MA Cenci and collaborators (Cenci et al., 1998; Cenci and Lundblad, 2007) and also reported by our group (Marti et al., 2012; Mela et al., 2012; Paolone et al., 2015). Rats were observed individually for 1 min every 20 min during the 3 h that followed an L-DOPA injection. Dyskinetic movements were classified into four subtypes based on their topographic distribution: (i) axial AIMs, i.e. twisted posture or choreiform twisting of the neck and upper body toward the side contralateral to the lesion; (ii) forelimb AIMs, i.e. jerky or dystonic movements of the contralateral forelimb and/or purposeless grabbing movements of the contralateral paw; (iii) orolingual AIMs, i.e. orofacial muscle twitching, empty masticatory movements and contralateral tongue protrusion. Each AIM subtype was rated from 0 to 4 on frequency and amplitude scales (Cenci and Lundblad, 2007). Dyskinesia score was calculated (in the induction phase and during the microdialysis sessions) as the product of frequency x amplitude scores (Cenci and Lundblad, 2007), and presented as cumulative axial, limb and orolingual (ALO) AIM score (values given in text) or separate score for each AIM subtype (figure panels A). The theoretical maximal total ALO AIM score for each animal was 432 during the induction phase (axial, limb and orolingual AIMs scored on a 0–4 intensity x amplitude scale, maximum score of 48 for each evaluation session, nine 20-min sessions), and 288 during microdialysis (six 20-min evaluation sessions). In addition to ALO AIMs, a fourth subtype of dyskinetic movements, known as locomotive AIMs, i.e. increased locomotion with contralateral side bias, was monitored and presented in figure panels A to improve the behavioral analysis.

2.4. Endogenous Glu and GABA analysis

Glu and GABA in the dialysate were measured by HPLC coupled with fluorometric detection as previously described (Mela et al., 2012; Paolone et al., 2015). Thirty microliters of o-phthaldialdehyde/mercaptoethanol reagent were added to 30 μl aliquots of sample, and 50 μl of the mixture were automatically injected (Triathlon autosampler; Spark Holland, Emmen, Netherlands) onto a 5-C18 Hypersil ODS analytical column (3 mm inner diameter, 10 cm length; Thermo-Fisher, USA) perfused at a flow rate of 0.48 ml/min (Jasco PU-2089 Plus quaternary pump; Jusco, Tokyo, Japan) with a mobile phase containing 0.1 M sodium acetate, 10% methanol and 2.2% tetrahydrofuran (pH 6.5). Glu and GABA were detected by means of a fluorescence spectrophotometer FP-2020 plus (Jasco, Tokyo, Japan) with the excitation and the emission wavelengths set at 370 and 450 nm respectively. Under these conditions, the limits of detection for Glu and GABA were ~ 1 nM and 0.5 nM, and their retention times were ~ 3.5 min and ~ 18.0 min, respectively. Chromatogram analysis was made by a blinded experimenter using a dedicated ChromNav software (Jasco, Tokyo, Japan).

2.5. TH analysis

Rats were sacrificed by an overdose of isoflurane. Striata were solubilized and homogenized in lysis buffer (RIPA buffer, protease and phosphatase inhibitor cocktail) and centrifuged at 18,000 x*g* for 15 min at 4 °C (Pisanò et al., 2020). Supernatants were collected and total protein levels were quantified using the bicinchoninic acid protein assay kit (Thermo Scientific). Thirty micrograms of protein per sample were separated by SDS-PAGE, transferred onto polyvinyldifluoride membrane and incubated overnight (4 °C) with the rabbit anti-TH primary antibody (Merck Millipore, AB152, 1:1000). Membranes were then washed and incubated with horseradish peroxidase-linked secondary antibody (Merck Millipore, goat anti-rabbit IgG HRP-conjugate 12–348, 1:4000). Immunoreactive proteins were visualized by enhanced chemiluminescence (ECL) detection kit (Pierce™ BCA Protein Assay Kit, Thermo Scientific or ECL+, GE Healthcare). Images were acquired and quantified using the ChemiDoc MP System and the ImageLab Software (Bio-Rad). Membranes were then stripped and reprobed with rabbit anti-α-tubulin antibody (Merck-Millipore 04–1117, 1:25000). Data were analyzed by densitometry and the optical density of TH protein band was normalized to α-tubulin levels.

2.6. Experimental design

After surgery, dyskinetic rats were randomized to L-DOPA or L-DOPA in combination with a mAChR ligand in Day 1 microdialysis session, and treatments were crossed in Day 2 session. For instance, rats received L-DOPA alone in Day 1 session and L-DOPA plus telenzepine in Day 2 session, in a counterbalanced design. We have previously shown that 24 h is sufficient time for drug washout (Mela et al., 2012; Paolone et al., 2015; Pisanò et al., 2020). To accelerate drug clearance at the end of reverse dialysis experiments, probes were flushed with Ringer solution for 30 min. Experimenters were blinded to treatments. The effect of mAChR ligands OFF L-DOPA was investigated in separate groups of rats. In this case, one rat received two different ligands, randomized in Day 1 and Day 2 sessions in a counterbalanced design.

Reverse dialysis of mAChR antagonists through the microdialysis probe allowed to deliver constant amount of compounds in the extracellular space at stable and pharmacologically selective levels, approximating the affinity values for the target receptor. This was accomplished by taking into account in vitro recovery, that approximates 10% for the 3 mm probe implanted in striatum. We therefore estimated that roughly one tenth of the nominal concentration of the compound in the perfusion Ringer would be delivered to the extracellular space. Considering the poor selectivity of mAChR antagonists, this approach might represent an advantage over classical microinjection protocols. Telenzepine is an M1 mAChR preferring antagonist, with an affinity of 1–3 nM for M1 mAChRs, a 2–5-fold selectivity for M1 over M4 mAChRs, and a 5–30-fold selectivity for M1 over M2, M3 and M5 mAChRs (Doods et al., 1987; Lazareno et al., 1990; Tanda et al., 2007). Telenzepine was perfused through the probe at 100 nM, in order to generate extracellular concentrations of ~10 nM (i.e. 3–10-fold greater than the affinity for M1 mAChRs). PD-102807 is an M4 mAChR preferring antagonist, with 7–28 nM affinity for M4 mAChRs, a 14–36-fold selectivity for M4 over M3 mAChRs, and 76–2600-fold selectivity for M4 over M1, M2 and M5 mAChRs (Bohme et al., 2002; Croy et al., 2016). PD102807 was perfused at 3 μM to generate extracellular concentrations 10–30 times greater than its affinity for M4 mAChRs but much lower than its affinity for M1, M2 and M5 mAChRs. Tropicamide is considered an M4 mAChR preferring antagonist, with an affinity of 15 nM for M4 mAChRs (Lazareno and Birdsall, 1993; Lazareno et al., 1990). However, its selectivity for M4 over M1, M2 and M3 mAChRs is only 3-fold greater (Lazareno and Birdsall, 1993; Lazareno et al., 1990). In addition, a more recent study (Croy et al., 2016) questioned even such a small pharmacological preference. Thus, we decided to infuse 100 nM tropicamide to generate concentrations just below the affinity value for M4 mAChRs. VU0152100 is an M4 mAChR PAM, that increased by 70-fold the ACh potency in stimulating Ca^{2+} responses at M4 chimeric mAChRs (Brady et al., 2008). VU0152100 does not bind to the M4 mAChR orthosteric site or potentiates ACh binding to the other muscarinic receptor subtypes, thus appearing very selective for M4 mAChRs (Brady et al., 2008). We perfused 100 μM VU0152100 through the probe to generate extracellular levels about 30 times higher than its M4 activity (EC_{50} 380 nM). AFDX-116 is an M2 mAChR preferring antagonist, showing nanomolar affinity for M2 mAChRs (pKi 6.7–7.5), 3–4-fold selectivity over M4 mAChRs, 4–10-fold selectivity over M1

mAChRs and > 10-fold selectivity over M5 mAChRs (Billard et al., 1995; Doods et al., 1987; Stoll et al., 2009). The concentration used for reverse dialysis (200 nM) was chosen based on a microdialysis study showing that perfusion of 100 nM AFDX-116 through the probe was capable of increasing by > 70% ACh levels in striatum (Billard et al., 1995). Based on the affinity values reported above, such concentration is expected to generate extracellular levels slightly below the highest affinity value found in functional studies (pKi 7.5)(Billard et al., 1995).

2.7. Data and statistical analysis

The data and statistical analysis comply with the recommendations on experimental design and analysis in pharmacology (Curtis et al., 2018). Since in microdialysis experiments basal amino acid levels can differ greatly from animal to animal, data were normalized as a percentage of baseline values to minimize experimental variability, as in our previous publications. Statistical analysis on neurochemical data was performed (Graphpad Prism 6.0) on area-under-the-curve values (AUC; calculated in the 100–220 min range) followed by the Newman-Keuls test for multiple comparisons. AIMs were statistically analyzed using the Mann-Whitney *U* test or the Kruskal-Wallis test followed by the Dunn test for multiple comparisons when more than two groups were compared. Cumulative ALO AIM scores were given in text whereas scores of each AIM subtype were presented separately in graph (figure panels A). Alpha was set at 0.05.

2.8. Materials

L-DOPA methyl ester, benserazide hydrochloride, tropicamide and VU0152100 were purchased from Sigma-Aldrich (S. Louis MO, USA), 6-OHDA hydrobromide, telenzepine, PD-102807 and AFDX-116 from Tocris (Bristol, UK). Telenzepine, PD-102807, tropicamide, AFDX-116 and VU-0152100 were dissolved in Ringer for local perfusion through the microdialysis probe. 6-OHDA was dissolved in ascorbate-saline for intracerebral injection, whereas all the other drugs were dissolved in saline and administered systemically at the volume of 1.0 ml/Kg body weight.

3. Results

3.1. Striatal perfusion of telenzepine alleviated LID and inhibited nigral GABA and striatal Glu release

In order to evaluate whether M1 mAChRs influence LID and its neurochemical correlates, the M1 mAChR preferring antagonist telenzepine was perfused at the 100 nM concentration through the probe implanted in striatum, starting from 40 min before systemic (s.c.) L-DOPA administration. Acute L-DOPA injection induced severe ALO AIM expression (74.50 ± 5.71), and co-administration of telenzepine reduced it by ~35% overall (50.38 ± 6.32; U = 10.50, $p = 0.022$), a significant reduction being observed for axial AIMs (Fig. 1A). Basal dialysate levels were 21.53 ± 2.61 nM and 65.90 ± 7.47 nM for GABA and Glu in SNr ($n = 24$ each), respectively, and 65.64 ± 7.27 nM (n = 24) for Glu in striatum. Basal dialysate levels of nigral GABA ($F_{6,227} = 1.16$; $p < 0.331$) and Glu ($F_{6,227} = 1.12$; $p < 0.303$), and striatal Glu ($F_{5,196} = 0.85$; $p < 0.521$) did not significantly differ among this and the following sets of microdialysis experiments, and, more in general, across all sets of microdialysis experiments. LID expression was accompanied by the rise of nigral GABA ($F_{3,28} = 6.60$, $p = 0.0016$; Fig. 1B) and Glu ($F_{3,28} = 6.18$, $p = 0.0023$; Fig. 1C), as well as striatal Glu ($F_{3,28} = 7.21$, $p = 0.0010$; Fig. 1D). Intrastriatal perfusion with telenzepine prevented the L-DOPA-induced rise of nigral GABA (Fig. 1B) and striatal Glu (Fig. 1D), but not nigral Glu (Fig. 1C). Since neurotransmitter levels following perfusion of Ringer alone remained stable around basal values throughout the experiment, to limit the number of animals used in accordance with the 3R principle, Ringer perfusion was not repeated in next experiments.

3.2. Striatal perfusion of PD-102807 and tropicamide alleviated LID and inhibited nigral GABA and Glu along with striatal Glu release

In order to evaluate whether striatal M4 mAChRs influence LID and its neurochemical correlates, the M4 mAChR preferring antagonists PD-102807 and tropicamide were perfused through the probe implanted in striatum. Basal dialysate levels in PD-102807 experiment were 19.19 ± 2.62 nM and 47.77 ± 3.42 nM for GABA and Glu in SNr, respectively ($n = 24$ each), and 41.38 ± 4.25 nM (n = 24) for Glu in striatum, whereas in tropicamide experiment were 22.04 ± 2.56 nM and 48.89 ± 5.04 nM for GABA and Glu in SNr, respectively (n = 24 each), and 38.51 ± 4.11 nM (n = 24) for Glu in striatum. PD-102807 (3 μM) reduced global ALO AIM expression from 70.75 ± 5.64 to 25.38 ± 6.64 (−65%; $n = 8$ each; U = 0.00, $p = 0.0009$), significantly attenuating limb, axial and orolingual AIMs (Fig. 2A). PD-102807 (3 μM) inhibited the L-DOPA-induced rise of SNr GABA ($F_{2,21} = 12.64$, $p = 0.0002$; Fig. 2B), SNr Glu ($F_{2,21} = 8.93$, p = 0.0016; Fig. 2C), and striatal Glu ($F_{2,21} = 14.04$, $p = 0.0001$; Fig. 2D). Likewise, tropicamide (100 nM) attenuated LID expression by ~40% overall (59.38 ± 8.54 vs 35.25 ± 4.29, n = 8 each; U = 24.50, $p = 0.0163$), with a significant effect on limb AIMs (Fig. 3A). Tropicamide also prevented the LID-associated rise of SNr GABA ($F_{2,21} = 8.04$, $p = 0.0025$; Fig. 3B), SNr Glu ($F_{2,21} = 7.91$; $p = 0.0027$; Fig. 3C) and striatal Glu ($F_{2,21} = 6.75$; $p = 0.0054$; Fig. 3D).

3.3. Striatal perfusion of VU0152100 alleviated LID and inhibited nigral GABA and striatal Glu release

A study in mice and non-human primates revealed that an M4 mAChR PAM palliated LID (Shen et al., 2015). To confirm this finding in rats, and investigate whether an M4 mAChR PAM modulated striato-nigral MSN activity in vivo, VU0152100 (100 μM) was perfused in striatum. Basal dialysate levels were 19.97 ± 2.91 nM and 77.25 ± 7.60 nM for GABA and Glu in SNr, respectively (n = 24 each), and 63.09 ± 7.30 nM (n = 24) for Glu in striatum. Striatal perfusion of VU0152100 reduced L-DOPA-induced dyskinetic movements from 67.38 ± 3.57 to 42.13 ± 7.30 (~40%, U = 7.50, $p = 0.0076$, $n = 8$), the effect being significant on orolingual AIMs (Fig. 4A). VU0152100 also prevented the LID-associated surge of nigral GABA ($F_{2,21} = 7.06$, $p = 0.0045$; Fig. 4B) and Glu ($F_{2,21} = 6.25$, $p = 0.0074$; Fig. 4C). However, as revealed by 2-way ANOVA on single time-points, the inhibition of nigral Glu release was delayed, becoming significant from the 180-min time-point (time $F_{9,210} = 3.73$ $p < 0.0002$, treatment $F_{2,210} = 18.06$ $p < 0.0001$, time x treatment interaction $F_{18,210} = 2.25$ $p < 0.0035$). Unlike the M4 mAChR preferential antagonists, intrastriatal VU0152100 did not affect the LID-associated increase of striatal Glu release ($F_{2,21} = 4.15$, $p = 0.0302$; Fig. 4D).

3.4. Striatal perfusion of AFDX-116 blocked the antidyskinetic effect of PD-102807

Striatal M4 mAChRs are predominantly located presynaptically on ChIs (autoreceptors) (Alcantara et al., 2001; Yan and Surmeier, 1996; Zhang et al., 2002) and postsynaptically on glutamatergic cortico-striatal terminals (Pancani et al., 2014) and striato-nigral MSNs (Bernard et al., 1992; Hersch et al., 1994). To investigate whether the behavioral and neurochemical effects induced by striatal perfusion of PD-102807 were due to pre- or postsynaptic mechanisms, we intrastriatally perfused PD-102807 in combination with the M2 mAChR preferring antagonist, AFDX-116 (100 nM). Indeed, this concentration of AFDX-116 has been shown to elevate striatal ACh levels (Billard et al., 1995; Galarraga et al., 1999) and affect MSNs postsynaptically

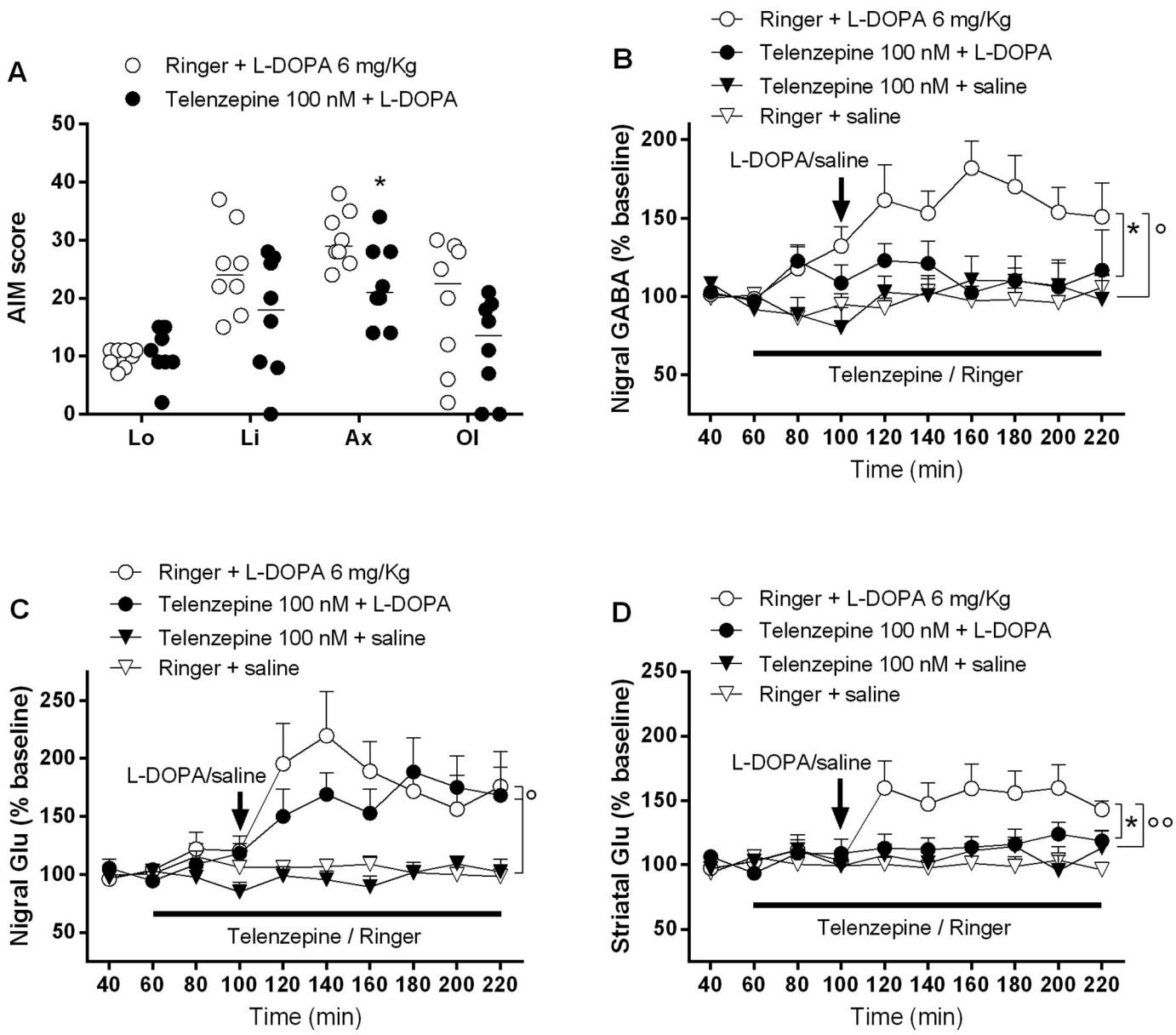

Fig. 1. Behavioral and neurochemical effects of reverse dialysis of telenzepine in the dopamine-depleted striatum of dyskinetic rats undergoing microdialysis. Dyskinetic rats were implanted with one probe in the lesioned dorsolateral striatum and another in ipsilateral substantia nigra reticulata (SNr). Twenty-four hours later, rats received an acute challenge with L-DOPA alone (6 mg/Kg plus 12 mg/Kg benserazide, s.c.) or in combination with telenzepine (100 nM) through the probe. Telenzepine perfusion started 40 min prior to L-DOPA administration and continued until the end of experiment. A group treated with telenzepine alone was also included. Axial (Ax), Limb (Li), Orolingual (Ol) and Locomotive (Lo) AIMs were scored for 1 min every 20 min over 120 min after L-DOPA administration. Points and medians refer to $n = 8$ rats per group (A). Dialysate samples were collected every 20 min for 120 min after L-DOPA administration, and GABA (B) and glutamate (Glu; C-D) levels in dialysates were monitored in SNr and striatum. Data are means ± SEM of 8 rats per group. Data were statistically analyzed using the Mann-Whitney test (AIM scores, arbitrary units; A) or ANOVA followed by the Newman-Keuls test (AUC values, B-D). *$p < 0.05$ different from Ringer + L-DOPA 6 mg/Kg; °p < 0.05, °°$p < 0.01$, different from Telenzepine 100 nM + saline.

(Galarraga et al., 1999). We reasoned that if the effects of PD-102807 were mediated by M4 autoreceptor blockade and elevation of striatal ACh levels, M2 autoreceptor blockade by AFDX-116 would further enhance or, at most, leave unchanged the effects of PD-102807. On the contrary, if the effects of PD-102807 were induced by postsynaptic M4 mAChR blockade, an increase of ACh levels would reverse them. Basal dialysate values were 14.59 ± 2.01 nM and 69.62 ± 8.37 nM for GABA and Glu in SNr, respectively ($n = 34$ each), and 60.02 ± 5.78 nM for Glu in striatum (n = 34). L-DOPA-induced AIMs expression (73.49 ± 1.03, $n = 8$) was not modified by striatal perfusion with AFDX-116 (76.50 ± 3.63, n = 8) or AFDX-116 plus PD-102807 (79.00 ± 3.23, n = 8; H = 4.29 $p = 0.11$; Fig. 5A). Consistently, in the presence of AFDX-116, PD-102807 failed to inhibit the LID-associated rise of nigral GABA ($F_{3,30} = 7.89$, $p = 0.0005$; Fig. 5B) or Glu ($F_{3,30} = 5.54$, $p = 0.0038$; Fig. 5C). Surprisingly enough, however, AFDX-116 failed to prevent the PD-102807 inhibition of the LID-associated increase of striatal Glu release (Fig. 5D).

3.5. Nigral perfusion of VU0152100 alleviated LID and its neurochemical correlates whereas nigral perfusion of PD-102807 was ineffective

Nigral M4 mAChRs, activated by cholinergic afferents from the PPN, exert a powerful modulation of D1 receptor signaling at the nerve terminals of striato-nigral MSNs in SNr (Moehle et al., 2017). To prove

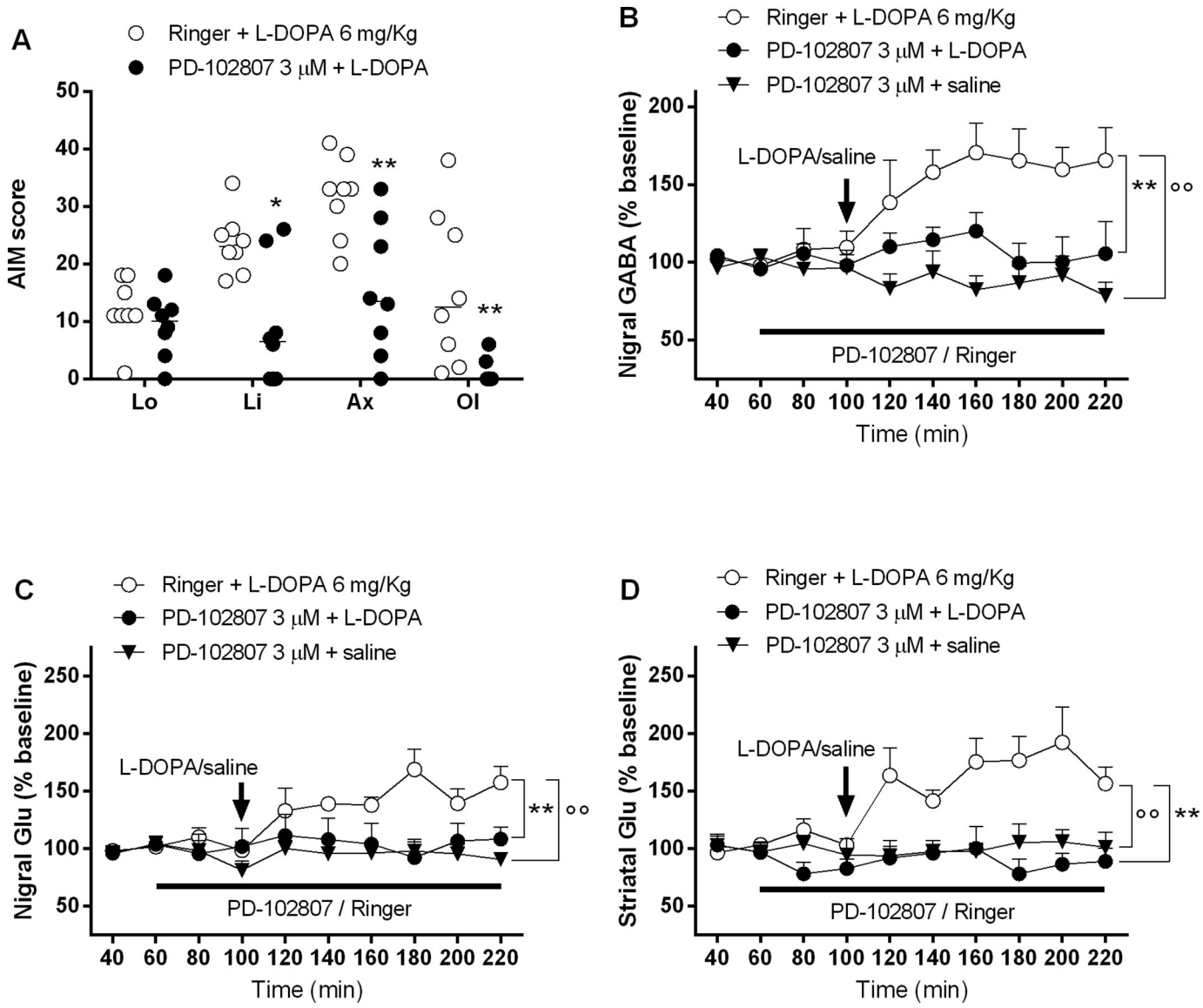

Fig. 2. Behavioral and neurochemical effects of reverse dialysis of PD-102807 in the dopamine-depleted striatum of dyskinetic rats undergoing microdialysis. Dyskinetic rats were implanted with one probe in the lesioned dorsolateral striatum and another in ipsilateral substantia nigra reticulata (SNr). Twenty-four hours later, rats received an acute challenge with L-DOPA alone (6 mg/Kg plus 12 mg/Kg benserazide, s.c.) or in combination with PD-102807 (3 μM) through the probe. PD-102807 perfusion started 40 min prior to L-DOPA administration and continued until the end of experiment. A group treated with PD-102807 alone was also included. Axial (Ax), Limb (Li), Orolingual (Ol) and Locomotive (Lo) AIMs were scored for 1 min every 20 min over 120 min after L-DOPA administration. Points and medians refer to n = 8 rats per group (A). Dialysate samples were collected every 20 min for 120 min after L-DOPA administration, and GABA (B) and glutamate (Glu; C-D) levels in dialysates were monitored in SNr and striatum. Data are means ± SEM of 8 rats per group. Data were statistically analyzed using the Mann-Whitney test (AIM scores, arbitrary units; A) or ANOVA followed by the Newman-Keuls test (AUC values, B-D). *p < 0.05, **p < 0.01 different from Ringer + L-DOPA 6 mg/Kg; °°p < 0.01, different from PD-102807 3 μM + saline.

that this modulation is relevant to LID, VU0152100 (100 μM) or PD-102807 (3 μM) were perfused through the probe implanted in SNr. Basal dialysate levels in VU0152100 experiment were 20.44 ± 2.58 nM and 73.05 ± 8.01 nM for GABA and Glu in SNr, respectively (n = 24 each), and 57.28 ± 4.72 nM for Glu in striatum (n = 24), whereas basal dialysate levels in PD-102807 experiment were 19.48 ± 2.01 nM and 67.32 ± 4.76 nM for GABA and Glu in SNr, respectively (n = 24 each). Dyskinetic movements induced by L-DOPA (69.75 ± 3.09, n = 8) were not affected by PD-102807 (80.00 ± 5.55) but inhibited (65%) by VU0152100 (30.75 ± 8.70, n = 8; H = 16.50 p = 0.0003). Both limb and axial AIMs were significantly reduced by VU0152100 (Fig. 6A). Intranigral VU0152100 also inhibited the LID-associated rise of nigral GABA ($F_{2,21}$ = 18.34, p < 0.0001; Fig. 6B), nigral Glu ($F_{2,21}$ = 4.99, p = 0.0168; Fig. 6C) and, unlike striatal perfusions, also striatal Glu ($F_{2,21}$ = 6.31, p = 0.0071; Fig. 6D). Consistent with its ineffectiveness in modulating LID, intranigral PD-102807 did not influence the LID-associated increase of nigral GABA ($F_{2,21}$ = 5.52, p = 0.0118; Fig. 6E) and Glu ($F_{2,21}$ = 4.860, p = 0.0184; Fig. 6F).

4. Discussion

An in vivo reverse dialysis approach was undertaken to deliver stable and target-selective concentrations of mAChR ligands in LID-relevant areas, in the attempt to circumvent the poor selectivity of mAChR antagonists and contribute to dissect out the role of striatal and nigral M1/M4 mAChRs in LID. Ligand concentrations were carefully selected based on a ~ 10% in vitro probe recovery and literature

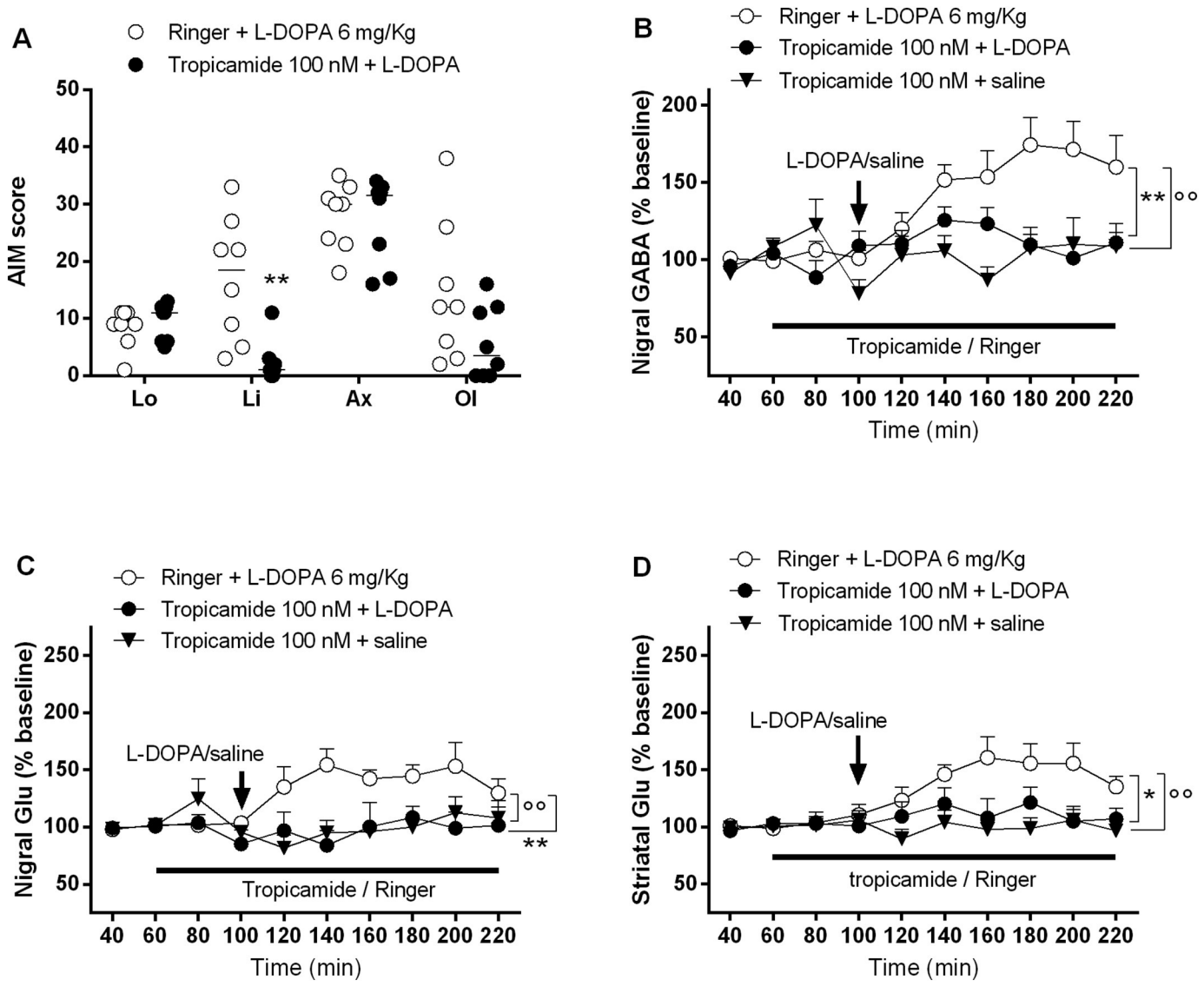

Fig. 3. Behavioral and neurochemical effects of reverse dialysis of tropicamide in the dopamine-depleted striatum of dyskinetic rats undergoing microdialysis. Dyskinetic rats were implanted with one probe in the lesioned dorsolateral striatum and another in ipsilateral substantia nigra reticulata (SNr). Twenty-four hours later, rats received an acute challenge with L-DOPA alone (6 mg/Kg plus 12 mg/Kg benserazide, s.c.) or in combination with tropicamide (100 nM) through the probe. Tropicamide perfusion started 40 min prior to L-DOPA administration and continued until the end of experiment. A group treated with tropicamide alone was also included. Axial (Ax), Limb (Li), Orolingual (Ol) and Locomotive (Lo) AIMs were scored for 1 min every 20 min over 120 min after L-DOPA administration. Points and medians refer to n = 8 rats per group (A). Dialysate samples were collected every 20 min for 120 min after L-DOPA administration, and GABA (B) and glutamate (Glu; C-D) levels in dialysates were monitored in SNr and striatum. Data are means ± SEM of 8 rats per group. Data were statistically analyzed using the Mann-Whitney test (AIM scores, arbitrary units; A) or ANOVA followed by the Newman-Keuls test (AUC values, B-D). *$p < 0.05$, **$p < 0.01$ different from Ringer + L-DOPA 6 mg/Kg; °°$p < 0.01$ different from Tropicamide 100 nM + saline.

affinity data obtained at cloned and/or native mAChRs. This approach has obvious limitations, related to the lack of information on the actual concentrations of the compounds in the extracellular space, and the true affinity values of mAChRs in native tissue and in vivo conditions. Moreover, reverse dialysis of a compound in a specific brain area might not fully replicate the effect of the same compound administered systemically. Nonetheless, this approach provides novel information on the role of M1 or M4 mAChRs in LID, integrating studies where mAChR ligands were administered systemically or locally microinjected in the brain, often without control over receptor selectivity.

4.1. Telenzepine in striatum

Intrastriatal reverse dialysis of the M1 mAChR preferring antagonist telenzepine attenuated LID expression and the accompanying rise of GABA in SNr. Previous in vivo microdialysis studies in dyskinetic rodents (Bido et al., 2011; Bido et al., 2015; Marti et al., 2012; Mela et al., 2012; Mela et al., 2007; Paolone et al., 2015) demonstrated that the rise of nigral GABA release which accompanies AIMs appearance reflects the activation of D1 receptor expressing striato-nigral MSNs. Therefore, telenzepine might inhibit LID through the blockade of M1 mAChRs located on striato-nigral MSNs. Indeed, M1 receptors increase striato-nigral and striato-pallidal MSN excitability through different mechanisms: i) closure of Kir2 and KCNQ (Kv7) K^+ channels (Shen et al., 2005), particularly in striato-pallidal MSNs (Shen et al., 2007); ii) enhancement of Ca^{2+}-currents through Ca_v1 channels, particularly in striato-nigral MSNs (Hernandez-Flores et al., 2015; Hernandez-Lopez et al., 1997; Perez-Garci et al., 2003); iii) facilitation of NMDA transmission (Calabresi et al., 1998) through persistent sodium currents (Carrillo-Reid et al., 2009); iv) inactivation of N- and P/Q Ca_v channels,

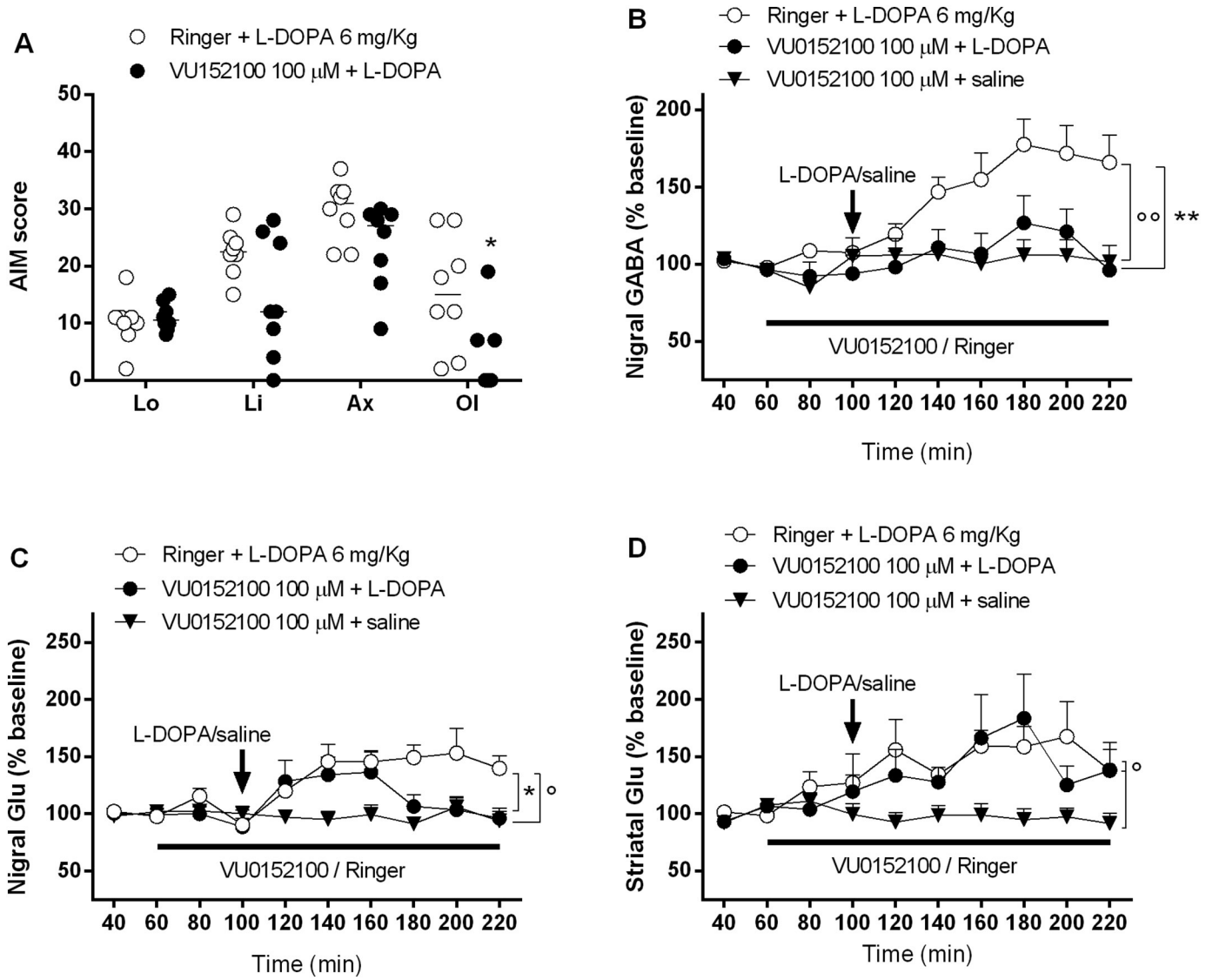

Fig. 4. Behavioral and neurochemical effects of reverse dialysis of VU0152100 in the dopamine-depleted striatum of dyskinetic rats undergoing microdialysis. Dyskinetic rats were implanted with one probe in the lesioned dorsolateral striatum and another in ipsilateral substantia nigra reticulata (SNr). Twenty-four hours later, rats received an acute challenge with L-DOPA alone (6 mg/Kg plus 12 mg/Kg benserazide, s.c.) or in combination with VU0152100 (100 μM) through the probe. VU0152100 perfusion started 40 min prior to L-DOPA administration and continued until the end of experiment. A group treated with VU0152100 alone was also included. Axial (Ax), Limb (Li), Orolingual (Ol) and Locomotive (Lo) AIMs were scored for 1 min every 20 min over 120 min after L-DOPA administration. Points and medians refer to n = 8 rats per group (A). Dialysate samples were collected every 20 min for 120 min after L-DOPA administration, and GABA (B) and glutamate (Glu; C-D) levels in dialysates were monitored in SNr and striatum. Data are means ± SEM of 8 rats per group. Data were statistically analyzed using the Mann-Whitney test (AIM scores, arbitrary units; A) or ANOVA followed by the Newman-Keuls test (AUC values, B-D). *p < 0.05; **p < 0.01 different from Ringer + L-DOPA 6 mg/Kg; °p < 0.05, °°p < 0.01, different from VU0152100 100 μM + saline.

leading to reduced GABA release from striatal interneurons (Perez-Rosello et al., 2005). To possibly confirm an action of telenzepine at M1 mAChRs on striato-nigral MSNs, systemic administration of the M1 mAChR preferring antagonist trihexyphenidyl inhibited dyskinesia triggered by the D1 receptor agonist SKF81297 (Chambers et al., 2019). In that study, however, systemic trihexyphenidyl worsened LID. This might be due to an interaction with extrastriatal M1 mAChRs and/or with striatal or extrastriatal non-M1 mAChRs. To further confirm an action along the striato-nigral direct pathway, intrastriatal telenzepine also reduced the LID-associated elevation of striatal Glu release (Brugnoli et al., 2016; Gardoni et al., 2018; Ostock et al., 2011; Paolone et al., 2015). In fact, elevation of striatal Glu release might result from stimulation of striato-nigral MSNs leading to activation of cortico-basal ganglia-thalamo-cortical loop (Mark et al., 2004; Marti et al., 2005) and cortico-striatal terminals (Ostock et al., 2011). However, Glu might also derive from striatal ChIs, which express the vesicular Glu transporter 3 (VGLUT3) (Kljakic et al., 2017). In fact, this pool of Glu contributes to both PD symptoms and LID (Divito et al., 2015; Gangarossa et al., 2016). Finally, Glu might also be released from thalamo-striatal terminals, which predominantly innervate striatal ChIs (Ding et al., 2010). This thalamic modulation plays a key role in regulating a cholinergic gating of cortico-striatal inputs, particularly setting a presynaptic M2 inhibitory/postsynaptic M1 excitatory mAChR balance over striato-pallidal MSNs activity (Ding et al., 2010; Sciamanna et al., 2012). Therefore, the reduction of striatal Glu in our model might not only reflect cortico-basal ganglia-thalamo-cortical loop inhibition but also normalization of ChIs activity and cortico/thalamo-striatal transmission. This might explain why striatal Glu release can dissociate from AIM appearance (Gardoni et al., 2018) (AFDX-116 and PD-102807 experiment in the present study) and impact behaviors beyond

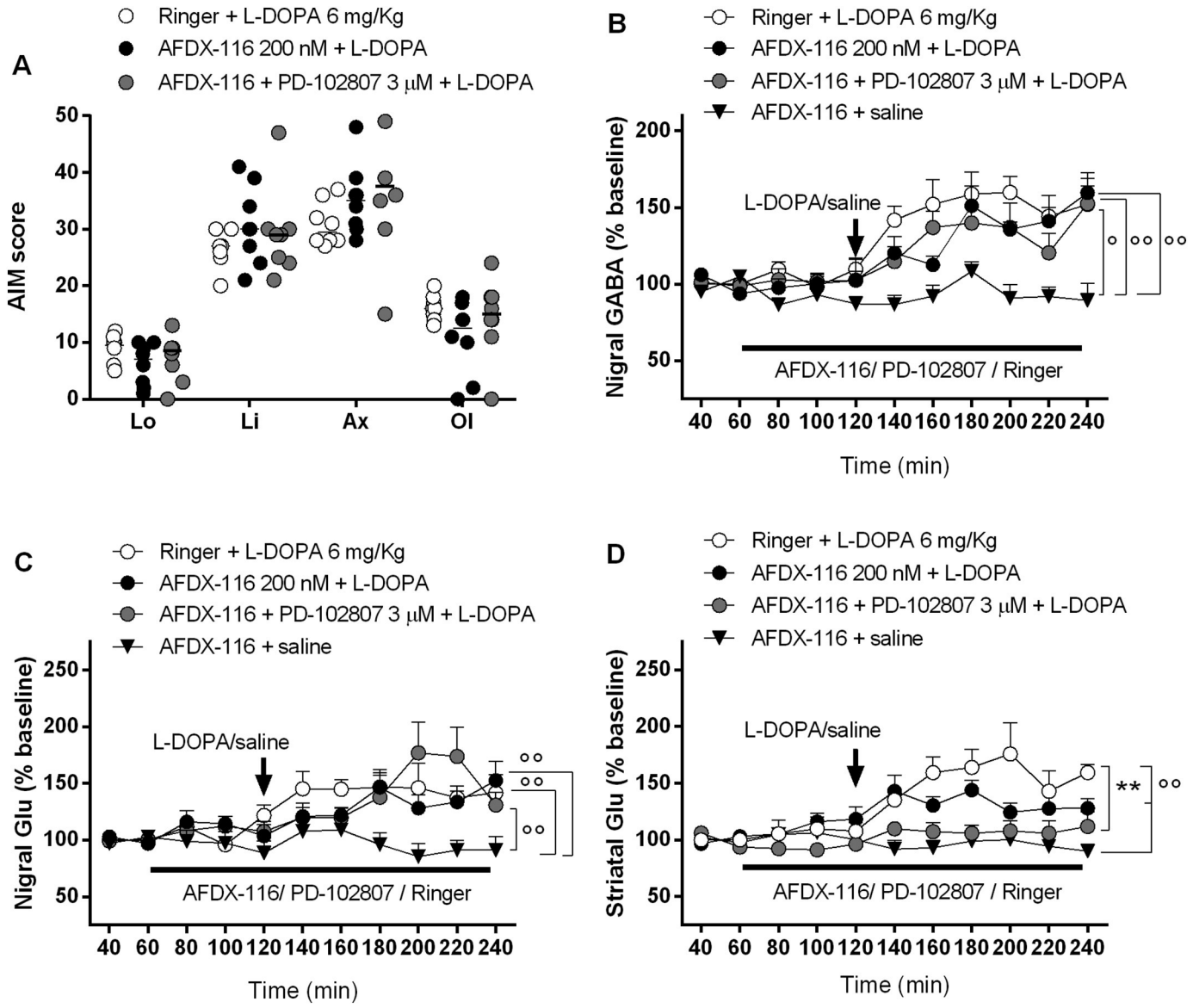

Fig. 5. Behavioral and neurochemical effects of reverse dialysis of AFDX-116 in the dopamine-depleted striatum of dyskinetic rats undergoing microdialysis. Dyskinetic rats were implanted with one probe in the lesioned dorsolateral striatum and another in ipsilateral substantia nigra reticulata (SNr). Twenty-four hours later, rats received an acute challenge with L-DOPA alone (6 mg/Kg plus 12 mg/Kg benserazide, s.c.) or in combination with AFDX-116 (200 nM) or AFDX-116 (200 nM) + PD-102807 (3 μM) through the probe. PD-102807 perfusion started 40 min prior to L-DOPA administration whereas perfusion with AFDX-116 started 60 min prior to L-DOPA or 20 min prior to PD-102807 and continued until the end of experiment. A group treated with AFDX-116 alone was also included. Axial (Ax), Limb (Li), Orolingual (Ol) and Locomotive (Lo) AIMs were scored for 1 min every 20 min over 120 min after L-DOPA administration. Points and medians refer to n = 8 rats per group (A). Dialysate samples were collected every 20 min for 120 min after L-DOPA administration, and GABA (B) and glutamate (C-D) levels in dialysates were monitored in striatum and SNr. Data are means ± SEM of 8 rats per group. Data were statistically analyzed using the Kruskal-Wallis test (AIM scores, arbitrary units; A) or ANOVA followed by the Newman-Keuls test (AUC values, B–D). *p < 0.05, **p < 0.01 different from Ringer + L-DOPA 6 mg/Kg; °p < 0.05; °°p < 0.01 different from AFDX-116 200 nM + saline (B-D).

dyskinesia. Indeed, high frequency stimulation of the subthalamic nucleus normalized the elevation of cortico-striatal glutamatergic transmission in dyskinetic rats, and this effect resulted in motor improvement but not LID attenuation (Gubellini et al., 2006). Moreover, inhibition of Glu release from thalamo-striatal terminals (via nAChR desensitization) reduced the firing of striato-pallidal MSNs and improved PD-related motor learning deficits (Tanimura et al., 2019). Due to the limitations of the microdialysis setting it was not possible to establish whether intrastriatal M1 mAChR blockade impacts on parkinsonian symptoms and/or the therapeutic effect of L-DOPA. Previous studies reported that M1 mAChR antagonists improve motor deficits in 6-OHDA hemilesioned mice (Ztaou et al., 2016) and enhance the L-DOPA antiparkinsonian effect in 6-OHDA hemilesioned rats (Chambers et al., 2019) likely acting at M1 mAChRs on striato-pallidal MSNs (Ztaou et al., 2016). The present study offers evidence of a behaviorally-relevant role of M1 mAChRs also along the striato-nigral MSNs.

4.2. VU0152100, PD-102807 and tropicamide in striatum

Consistent with previous finding that an M4 mAChR PAM VU0467154 attenuated LID and LID-associated aberrant plasticity at striato-nigral MSNs in mice and non-human primates (Shen et al., 2015), reverse dialysis of VU0152100 in striatum reduced LID and striato-nigral MSN activation in vivo. Quite unexpectedly, this pattern was replicated by reverse dialysis of the M4 mAChR preferring antagonists PD-102807 and tropicamide, paradoxically suggesting that

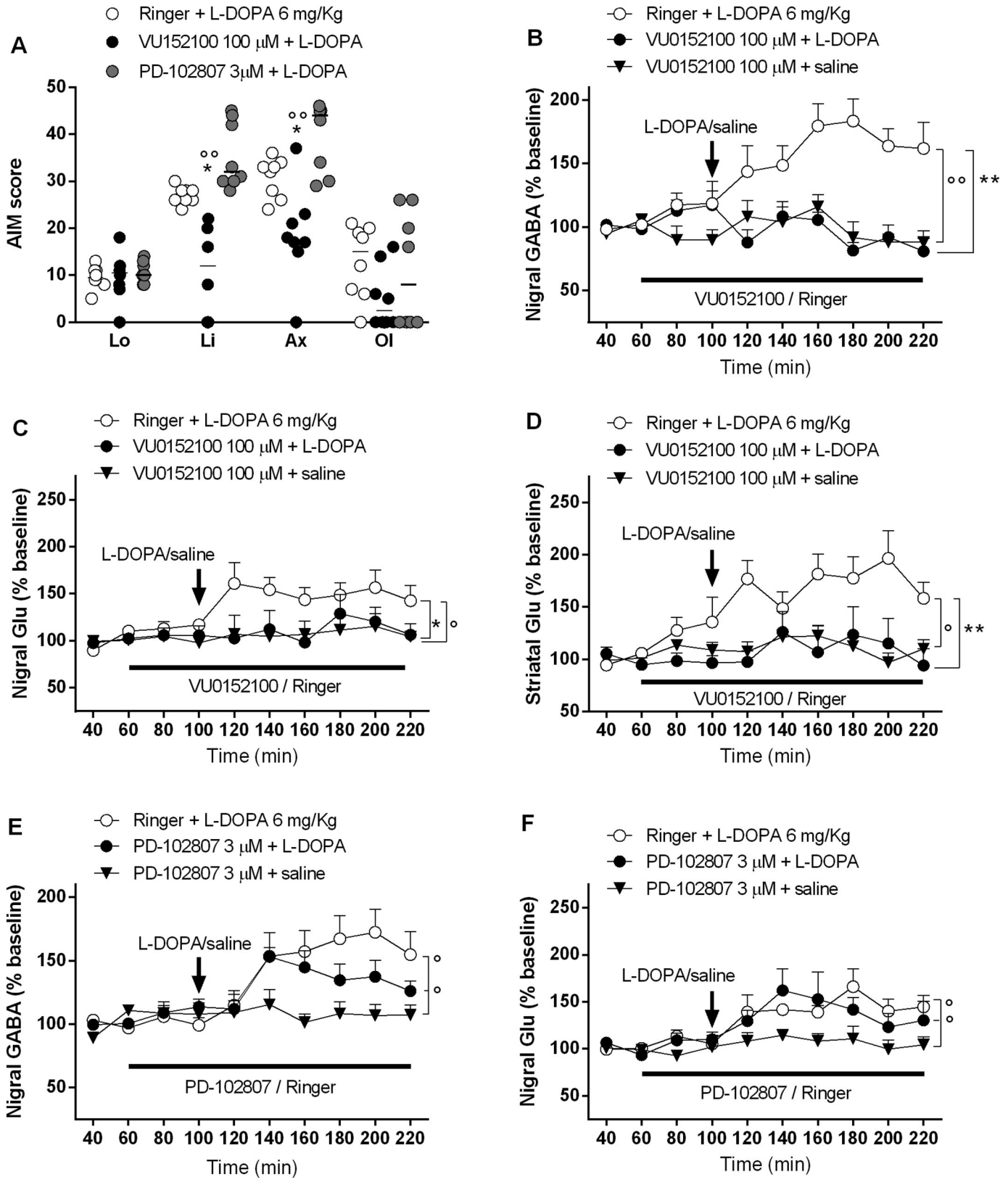

(caption on next page)

M4 mAChR stimulation and blockade regulate LID and LID-associated pathways in a similar way. The neurochemical patterns of VU0152100 and M4 mAChR antagonists, however, were not overlapping, possibly indicating that different sets of striatal M4 mAChR are involved. Striatal M4 mAChRs are expressed presynaptically on ChIs, where they operate as autoreceptors (Bonsi et al., 2008; Zhang et al., 2002), and post-synaptically on glutamatergic terminals, where they inhibit Glu release (Pancani et al., 2014), and striato-nigral MSNs, where they modulate D1 receptor signaling, Ca^{2+} channels, NMDA currents, and also release endocannabinoids that retrogradely modulate DA release (Moehle and

Fig. 6. Behavioral and neurochemical effects of reverse dialysis of VU0152100 or PD-102807 in the substantia nigra pars reticulata (SNr) of dyskinetic rats undergoing microdialysis. Dyskinetic rats were implanted with one probe in the lesioned dorsolateral striatum and another in ipsilateral SNr. Twenty-four hours later, rats received an acute challenge with L-DOPA alone (6 mg/Kg plus 12 mg/Kg benserazide, s.c.) or in combination with VU0152100 (100 μM) or PD-102807 (3 μM) through the nigral probe. VU0152100 or PD-102807 perfusion started 40 min prior to L-DOPA administration and continued until the end of experiment. A group treated with VU0152100 or PD-102807 alone were also included. Axial (Ax), Limb (Li), Orolingual (Ol) and Locomotive (Lo) AIMs were scored for 1 min every 20 min over 120 min after L-DOPA administration. Points and medians refer to n = 8 rats per group (A). Dialysate samples were collected every 20 min for 120 min after L-DOPA administration, and GABA (B, E) and glutamate (Glu; C,D,F—) levels in dialysates were monitored in SNr or striatum. Data are means ± SEM of 8 rats per group. Data were statistically analyzed using the Kruskal-Wallis test (AIM scores, arbitrary units; A) or ANOVA followed by the Newman-Keuls test (AUC values, B—F) *p < 0.05, **p < 0.01 different from Ringer + L-DOPA 6 mg/Kg; °p < 0.05; °°p < 0.01 different from VU0152100 100 μM + saline (B-D) or PD-102807 3 μM + saline (E-F).

Conn, 2019). Since PD-102807 concentrations were chosen to generate extracellular levels (~300 nM) well below the affinity for M1 mAChRs (1.3–1.6 μM) (Bohme et al., 2002; Croy et al., 2016), it is unlikely that the effects of PD-102807 are due to an interaction with M1 mAChRs. Opposite actions have been described for postsynaptic M4 mAChRs at striato-nigral MSNs. In dissociated neurons, M4 mAChR stimulation enhanced striato-nigral MSN excitability via the opening of Ca_V1 channels, thus facilitating a subsequent stimulation induced by a D1 receptor agonist (Hernandez-Flores et al., 2015). This is consistent with the increase of L-type Ca^{2+} currents mediated by M4 mAChRs in atrial cells (Pemberton and Jones, 1995). Conversely, in striatal slices a negative interaction between M4 mAChRs and D1 receptors at striato-nigral MSNs was described, which was relevant for the modulation of cAMP production, Ca^{2+} influx via dendritic NMDA receptors, and LTP (Shen et al., 2015). Consistent with a negative M4 mAChR regulation of striato-nigral MSN activity, constitutive M4 mAChR knock-out mice showed enhanced basal and D1 agonist stimulated motor activity (Gomeza et al., 1999) whereas M4 mAChR blockade improved sensorimotor deficits in 6-OHDA hemilesioned mice (Ztaou et al., 2016). Conversely, in line with a postsynaptic facilitatory action of M4 mAChRs at striato-nigral MSNs in LID (Chambers et al., 2019; Hernandez-Flores et al., 2015), we showed that PD-102807 and tropicamide inhibited dyskinetic movements along with the LID-associated elevation of nigral and striatal GABA and Glu levels. In fact, this neurochemical profile was shared by intrastriatal SCH23390 (Mela et al., 2012), which blocks D1 receptors on striato-nigral MSNs. Moreover, AFDX-116 counteracted the PD-102807 inhibition of LID and LID-associated nigral GABA release. This data could be interpreted as if the elevation of striatal ACh levels produced by M2 autoreceptor blockade surmounted the blockade of postsynaptic M4 mAChRs and/or overstimulated postsynaptic M1 mAChRs, thereby functionally counteracting the effects of PD-102807. Alternatively, the possibility should be considered that an elevation of the cholinergic tone leads to activation and desensitization of nAChRs, causing LID to subside (Quik et al., 2015). Finally, an fMRI study revealed that systemic M4 mAChR PAMs did not affect the D1 agonist induced changes in cerebral blood volume (CBV) in striatum, a hemodynamic response reflecting changes in neuronal activity, while inhibiting the amphetamine-induced CBV changes and DA release in the same area (Byun et al., 2014). Thus, the main site of action of M4 mAChR PAMs in striatum has been proposed to be presynaptic, i.e. the modulation of DA release, and not postsynaptic (Moehle and Conn, 2019; Moehle et al., 2017). We can therefore speculate that VU0152100 might reduce LID and MSN overactivation via presynaptic mechanisms, e.g. by inhibiting ectopic DA release from serotonergic terminals, the predominant site of L-DOPA conversion to DA in the DA-depleted striatum (Bastide et al., 2015), or by rescuing M4 autoreceptor function in ChIs, which is dampened due to upregulation of RGS4 proteins (Shen et al., 2015). However, since neither M4 mAChR blockade (Chambers et al., 2019) or stimulation (Shen et al., 2015) affected the therapeutic effect of L-DOPA, it is conceivable that the antidyskinetic effect of VU0152100 is mediated by the rescue of M4 autoreceptor function. The failure of intrastriatal M4 PAM VU0152100 in modulating striatal Glu release would rule out the possibility that the inhibitory control operated by M4 mAChRs on Glu terminals (Pancani et al., 2014) contributes to the antidyskinetic effect of VU0152100.

4.3. VU0152100 and PD-102807 in SNr

Reverse dialysis of VU0152100 in SNr prevented LID and the accompanying rise of nigral GABA release. This is consistent with the findings that the M4 mAChR PAM VU0467154 inhibited the D1 agonist induced GABA release from striato-nigral MSNs terminals in vitro, and CBV in SNr in vivo (Moehle et al., 2017). The profile of intranigral VU0152111 confirms the role of the cholinergic afferents arising from PPN in the modulation of D1 signaling in SNr (Moehle et al., 2017) and shows that this modulation shapes LID. Indeed, the neurochemical responses to intranigral VU0152100, also considering the inhibition of striatal Glu, are consistent with the view that M4 mAChR stimulation inhibits GABA release from striato-nigral MSN terminals in vivo, thus limiting the overinhibition of nigro-thalamic GABAergic neurons (i.e. the nigral output) associated with LID. In vitro electrophysiological experiments in nigral slices showed that the M4 mAChR inhibition of nigral D1 signaling and GABA release is tonically active (Moehle et al., 2017). However, in the present in vivo model, blockade of nigral M4 mAChR with PD-102807 did not alter nigral LID and nigral GABA and Glu release, suggesting that endogenous ACh acting at nigral M4 mAChRs does not contribute to LID. Nonetheless, we should consider that LID is already maximal in these animals, thus making it difficult to capture further AIM increases.

4.4. Concluding remarks

Consistent with previous evidence that unspecific muscarinic antagonists dicyclomine and atropine prevented LID expression (Bordia et al., 2016; Ding et al., 2011), intrastriatal telenzepine, PD-102807 and tropicamide attenuated LID and striato-nigral MSNs activation, indicating that both M1 and M4 receptors contribute to LID. Moreover, in keeping with the view that mAChRs also mediate an inhibitory action of endogenous ACh on LID (Bordia et al., 2016), potentiation of cholinergic transmission at striatal M4 mAChRs resulted in significant inhibition of LID and striato-nigral MSN activation. Therefore, M4 mAChRs can both facilitate and inhibit LID. During LID, endogenous ACh seems to facilitate LID acting at striatal postsynaptic M4 mAChRs. However, pharmacological potentiation of different populations of striatal M4 mAChRs (possibly presynaptically located on dopaminergic terminals or ChIs) would unmask an overwhelming inhibitory control over LID. Moreover, consistent with previous evidence that PPN cholinergic inputs to SNr affect basal ganglia functions (Moehle et al., 2017; Xiao et al., 2016), the present study shows for the first time that stimulation of M4 mAChRs in SNr inhibited LID and nigral output in vivo. Altogether, this study provides in vivo evidence for powerful, multilevel M4 mAChR modulation of striato-nigral MSNs, reinforcing the view that the M4 mAChR is a promising target in LID therapy (Moehle and Conn, 2019).

Funding

This work was supported by a grant from the Italian Ministry of University to M.M. (PRIN 2010–2011 #2010AHHP5H).

Credit author statement

Alberto Brugnoli: Conceptualization; Data curation; Formal analysis; Funding acquisition; Investigation; Methodology; Roles/Writing - original draft; Writing - review & editing.

Clarissa Anna Pisanò: Data curation; Formal analysis; Investigation; Methodology; Writing - review & editing.

Michele Morari: Conceptualization; Data curation; Formal analysis; Funding acquisition; Project administration; Resources; Supervision; Roles/Writing - original draft; Writing - review & editing.

Declaration of Competing Interest

AB is postdoc at the University of Ferrara, CAP is PhD student at the University of Ferrara, MM is employed by the University of Ferrara. The authors declare no competing financial interests.

Appendix A. Supplementary data

Supplementary data to this article can be found online at https://doi.org/10.1016/j.nbd.2020.105044.

References

Alcantara, A.A., et al., 2001. Muscarinic m1 and m2 receptor proteins in local circuit and projection neurons of the primate striatum: anatomical evidence for cholinergic modulation of glutamatergic prefronto-striatal pathways. J. Comp. Neurol. 434, 445–460.

Bastide, M.F., et al., 2015. Pathophysiology of L-dopa-induced motor and non-motor complications in Parkinson's disease. Prog. Neurobiol. 132, 96–168.

Bernard, V., et al., 1992. Phenotypical characterization of the rat striatal neurons expressing muscarinic receptor genes. J. Neurosci. 12, 3591–3600.

Bido, S., et al., 2011. Amantadine attenuates levodopa-induced dyskinesia in mice and rats preventing the accompanying rise in nigral GABA levels. J. Neurochem. 118, 1043–1055.

Bido, S., et al., 2015. Differential involvement of Ras-GRF1 and Ras-GRF2 in L-DOPA-induced dyskinesia. Ann Clin Transl Neurol. 2, 662–678.

Billard, W., et al., 1995. Identification of the primary muscarinic autoreceptor subtype in rat striatum as m2 through a correlation of in vivo microdialysis and in vitro receptor binding data. J. Pharmacol. Exp. Ther. 273, 273–279.

Bohme, T.M., et al., 2002. Synthesis and pharmacology of benzoxazines as highly selective antagonists at M(4) muscarinic receptors. J. Med. Chem. 45, 3094–3102.

Bonsi, P., et al., 2008. Loss of muscarinic autoreceptor function impairs long-term depression but not long-term potentiation in the striatum. J. Neurosci. 28, 6258–6263.

Bordia, T., Perez, X.A., 2019. Cholinergic control of striatal neurons to modulate L-dopa-induced dyskinesias. Eur. J. Neurosci. 49, 859–868.

Bordia, T., et al., 2016. Optogenetic activation of striatal cholinergic interneurons regulates L-dopa-induced dyskinesias. Neurobiol. Dis. 91, 47–58.

Brady, A.E., et al., 2008. Centrally active allosteric potentiators of the M4 muscarinic acetylcholine receptor reverse amphetamine-induced hyperlocomotor activity in rats. J. Pharmacol. Exp. Ther. 327, 941–953.

Brugnoli, A., et al., 2016. Genetic deletion of Rhes or pharmacological blockade of mTORC1 prevent striato-nigral neurons activation in levodopa-induced dyskinesia. Neurobiol. Dis. 85, 155–163.

Byun, N.E., et al., 2014. Antipsychotic drug-like effects of the selective M4 muscarinic acetylcholine receptor positive allosteric modulator VU0152100. Neuropsychopharmacology. 39, 1578–1593.

Calabresi, P., et al., 1998. Endogenous ACh enhances striatal NMDA-responses via M1-like muscarinic receptors and PKC activation. Eur. J. Neurosci. 10, 2887–2895.

Calabresi, P., et al., 2000. Acetylcholine-mediated modulation of striatal function. Trends Neurosci. 23, 120–126.

Carrillo-Reid, L., et al., 2009. Muscarinic enhancement of persistent sodium current synchronizes striatal medium spiny neurons. J. Neurophysiol. 102, 682–690.

Cenci, M. A., Lundblad, M., 2007. Ratings of L-DOPA-induced dyskinesia in the unilateral 6-OHDA lesion model of Parkinson's disease in rats and mice. Curr Protoc Neurosci. Chapter 9, unit 9 25.

Cenci, M.A., et al., 1998. L-DOPA-induced dyskinesia in the rat is associated with striatal overexpression of prodynorphin- and glutamic acid decarboxylase mRNA. Eur. J. Neurosci. 10, 2694–2706.

Chambers, N.E., et al., 2019. Effects of muscarinic acetylcholine m1 and m4 receptor blockade on dyskinesia in the hemi-parkinsonian rat. Neuroscience. 409, 180–194.

Croy, C.H., et al., 2016. Characterization of PCS1055, a novel muscarinic M4 receptor antagonist. Eur. J. Pharmacol. 782, 70–76.

Curtis, M.J., et al., 2018. Experimental design and analysis and their reporting II: updated and simplified guidance for authors and peer reviewers. Br. J. Pharmacol. 175, 987–993.

Ding, J.B., et al., 2010. Thalamic gating of corticostriatal signaling by cholinergic interneurons. Neuron. 67, 294–307.

Ding, Y., et al., 2011. Enhanced striatal cholinergic neuronal activity mediates L-DOPA-induced dyskinesia in parkinsonian mice. Proc. Natl. Acad. Sci. U. S. A. 108, 840–845.

Divito, C.B., et al., 2015. Loss of VGLUT3 produces circadian-dependent Hyperdopaminergia and ameliorates motor dysfunction and l-Dopa-mediated Dyskinesias in a model of Parkinson's disease. J. Neurosci. 35, 14983–14999.

Doods, H.N., et al., 1987. Selectivity of muscarinic antagonists in radioligand and in vivo experiments for the putative M1, M2 and M3 receptors. J. Pharmacol. Exp. Ther. 242, 257–262.

Espay, A.J., et al., 2018. Levodopa-induced dyskinesia in Parkinson disease: current and evolving concepts. Ann. Neurol. 84, 797–811.

Galarraga, E., et al., 1999. Cholinergic modulation of neostriatal output: a functional antagonism between different types of muscarinic receptors. J. Neurosci. 19, 3629–3638.

Gangarossa, G., et al., 2016. Role of the atypical vesicular glutamate transporter VGLUT3 in l-DOPA-induced dyskinesia. Neurobiol. Dis. 87, 69–79.

Gardoni, F., et al., 2018. Safinamide modulates striatal glutamatergic Signaling in a rat model of levodopa-induced dyskinesia. J. Pharmacol. Exp. Ther. 367, 442–451.

Gomeza, J., et al., 1999. Enhancement of D1 dopamine receptor-mediated locomotor stimulation in M(4) muscarinic acetylcholine receptor knockout mice. Proc. Natl. Acad. Sci. U. S. A. 96, 10483–10488.

Gubellini, P., et al., 2006. Chronic high-frequency stimulation of the subthalamic nucleus and L-DOPA treatment in experimental parkinsonism: effects on motor behaviour and striatal glutamate transmission. Eur. J. Neurosci. 24, 1802–1814.

Hernandez-Flores, T., et al., 2015. Modulation of direct pathway striatal projection neurons by muscarinic M(4)-type receptors. Neuropharmacology. 89, 232–244.

Hernandez-Lopez, S., et al., 1997. D1 receptor activation enhances evoked discharge in neostriatal medium spiny neurons by modulating an L-type Ca2+ conductance. J. Neurosci. 17, 3334–3342.

Hersch, S.M., et al., 1994. Distribution of m1-m4 muscarinic receptor proteins in the rat striatum: light and electron microscopic immunocytochemistry using subtype-specific antibodies. J. Neurosci. 14, 3351–3363.

Kljakic, O., et al., 2017. Cholinergic/glutamatergic co-transmission in striatal cholinergic interneurons: new mechanisms regulating striatal computation. J. Neurochem. 142 (Suppl. 2), 90–102.

Lazareno, S., Birdsall, N.J., 1993. Pharmacological characterization of acetylcholine-stimulated [35S]-GTP gamma S binding mediated by human muscarinic m1-m4 receptors: antagonist studies. Br. J. Pharmacol. 109, 1120–1127.

Lazareno, S., et al., 1990. Characterization of muscarinic M4 binding sites in rabbit lung, chicken heart, and NG108-15 cells. Mol. Pharmacol. 38, 805–815.

Mark, K.A., et al., 2004. High-dose methamphetamine acutely activates the striatonigral pathway to increase striatal glutamate and mediate long-term dopamine toxicity. J. Neurosci. 24, 11449–11456.

Marti, M., et al., 2005. Striatal glutamate release evoked in vivo by NMDA is dependent upon ongoing neuronal activity in the substantia nigra, endogenous striatal substance P and dopamine. J. Neurochem. 93, 195–205.

Marti, M., et al., 2007. The nociceptin/orphanin FQ receptor antagonist J-113397 and L-DOPA additively attenuate experimental parkinsonism through overinhibition of the nigrothalamic pathway. J. Neurosci. 27, 1297–1307.

Marti, M., et al., 2012. Nociceptin/orphanin FQ receptor agonists attenuate L-DOPA-induced dyskinesias. J. Neurosci. 32, 16106–16119.

Mela, F., et al., 2007. Antagonism of metabotropic glutamate receptor type 5 attenuates l-DOPA-induced dyskinesia and its molecular and neurochemical correlates in a rat model of Parkinson's disease. J. Neurochem. 101, 483–497.

Mela, F., et al., 2012. In vivo evidence for a differential contribution of striatal and nigral D1 and D2 receptors to L-DOPA induced dyskinesia and the accompanying surge of nigral amino acid levels. Neurobiol. Dis. 45, 573–582.

Moehle, M.S., Conn, P.J., 2019. Roles of the M4 acetylcholine receptor in the basal ganglia and the treatment of movement disorders. Mov. Disord. 34, 1089–1099.

Moehle, M.S., et al., 2017. Cholinergic projections to the substantia Nigra pars Reticulata inhibit dopamine modulation of basal ganglia through the M4 muscarinic receptor. Neuron. 96 (1358–1372), e4.

Morari, M., et al., 1996. Functional neuroanatomy of the nigrostriatal and striatonigral pathways as studied with dual probe microdialysis in the awake rat—I Effects of perfusion with tetrodotoxin and low-calcium medium. Neuroscience. 72, 79–87.

Ostock, C.Y., et al., 2011. Role of the primary motor cortex in L-Dopa-induced dyskinesia and its modulation by 5-HT1A receptor stimulation. Neuropharmacology. 61, 753–760.

Pancani, T., et al., 2014. M4 mAChR-mediated modulation of glutamatergic transmission at corticostriatal synapses. ACS Chem. Neurosci. 5, 318–324.

Paolone, G., et al., 2015. Eltoprazine prevents levodopa-induced dyskinesias by reducing striatal glutamate and direct pathway activity. Mov. Disord. 30, 1728–1738.

Paxinos, G., Watson, C., 1986. The rat brain in stereotaxic coordinates. Academic Press, Sydney; Orlando.

Pemberton, K.E., Jones, S.V., 1995. Enhancement of an L-type calcium current in AtT-20 cells; a novel effect of the m4 muscarinic receptor. Pflugers Arch. 429, 699–707.

Perez-Garci, E., et al., 2003. The role of Ca2+ channels in the repetitive firing of striatal projection neurons. Neuroreport. 14, 1253–1256.

Perez-Rosello, T., et al., 2005. Cholinergic control of firing pattern and neurotransmission in rat neostriatal projection neurons: role of CaV2.1 and CaV2.2 Ca2+ channels. J. Neurophysiol. 93, 2507–2519.

Pisani, A., et al., 2007. Re-emergence of striatal cholinergic interneurons in movement disorders. Trends Neurosci. 30, 545–553.

Pisanò, C.A., et al., 2020. Safinamide inhibits in vivo glutamate release in a rat model of Parkinson's disease. Neuropharmacology. 167.

Quik, M., et al., 2015. Nicotine and nicotinic receptor drugs: potential for Parkinson's

disease and drug-induced movement disorders. Int. Rev. Neurobiol. 124, 247–271.
Sciamanna, G., et al., 2012. Cholinergic dysfunction alters synaptic integration between thalamostriatal and corticostriatal inputs in DYT1 dystonia. J. Neurosci. 32, 11991–12004.
Shen, W., et al., 2005. Cholinergic suppression of KCNQ channel currents enhances excitability of striatal medium spiny neurons. J. Neurosci. 25, 7449–7458.
Shen, W., et al., 2007. Cholinergic modulation of Kir2 channels selectively elevates dendritic excitability in striatopallidal neurons. Nat. Neurosci. 10, 1458–1466.
Shen, W., et al., 2015. M4 muscarinic receptor Signaling ameliorates striatal plasticity deficits in models of L-DOPA-induced dyskinesia. Neuron. 88, 762–773.
Stoll, C., et al., 2009. Functional characterization of muscarinic autoreceptors in rat and human neocortex. J. Neurochem. 110, 837–847.
Tanda, G., et al., 2007. Effects of muscarinic M1 receptor blockade on cocaine-induced elevations of brain dopamine levels and locomotor behavior in rats. J. Pharmacol. Exp. Ther. 321, 334–344.
Tanimura, A., et al., 2019. Cholinergic interneurons amplify Thalamostriatal excitation of striatal indirect pathway neurons in Parkinson's disease models. Neuron. 101 (444–458), e6.
Won, L., et al., 2014. Striatal cholinergic cell ablation attenuates L-DOPA induced dyskinesia in parkinsonian mice. J. Neurosci. 34, 3090–3094.
Xiao, C., et al., 2016. Cholinergic Mesopontine signals govern locomotion and reward through dissociable midbrain pathways. Neuron. 90, 333–347.
Yan, Z., Surmeier, D.J., 1996. Muscarinic (m2/m4) receptors reduce N- and P-type Ca2+ currents in rat neostriatal cholinergic interneurons through a fast, membrane-delimited. G-protein pathway. J Neurosci. 16, 2592–2604.
Zhang, W., et al., 2002. Characterization of central inhibitory muscarinic autoreceptors by the use of muscarinic acetylcholine receptor knock-out mice. J. Neurosci. 22, 1709–1717.
Ztaou, S., et al., 2016. Involvement of striatal cholinergic interneurons and M1 and M4 muscarinic receptors in motor symptoms of Parkinson's disease. J. Neurosci. 36, 9161–9172.